Pacing-induced spatiotemporal dynamics can be exploited to improve reentry termination efficacy

Trine Krogh-Madsen[1] and David J. Christini[1,2]
[1]*Department of Medicine, Greenberg Division of Cardiology, Weill Cornell Medical College, New York, New York 10021, USA*
[2]*Department of Physiology and Biophysics, Weill Cornell Medical College, New York, New York 10021, USA*
(Received 20 March 2009; revised manuscript received 30 May 2009; published 21 August 2009)

Some potentially fatal cardiac arrhythmias may be terminated by a series of premature stimuli. Monomorphic ventricular tachycardia, which may be modeled as an excitation wave traveling around in a ring, is one such arrhythmia. We investigated the mechanisms and requirements for termination of such reentry using an ionic cardiac ring model. Termination requires conduction block, which in turn is facilitated by spatial dispersion in repolarization and recovery time. When applying short series of two or three stimuli, we found that for conduction block to robustly occur, the magnitude of the spatial gradient in recovery time must exceed a critical value of 20 ms/cm. Importantly, the required spatial gradient can be induced in this homogeneous system by the dynamics of the stimulus-induced waves—we show analytically the necessary conditions. Finally, we introduce a type of pacing protocol, the "aggressive ramp," which increases the termination efficacy by exploiting such pacing-induced heterogeneities. This technique, which is straightforward to implement, may therefore have important clinical implications.

DOI: 10.1103/PhysRevE.80.021924 PACS number(s): 87.19.Hh, 87.10.−e, 05.45.−a

I. INTRODUCTION

Reentrant cardiac arrhythmias, such as monomorphic ventricular tachycardia, occur when tissue is repeatedly activated by a self-sustained wave, e.g., one circulating an anatomical obstacle. Such cardiac reentry can often be terminated by a rapid sequence of applied stimuli. One possible explanation for such termination is unidirectional block, in which a stimulus induces a wave that travels only in the direction opposite (retrograde) to the reentrant wave. When these two waves collide, they mutually annihilate, terminating the reentry [1,2].

The time interval in which a stimulus leads to termination of the reentrant activity is termed the vulnerable window. Stable reentry in cardiac ionic models typically has a vulnerable window of 1–2 ms when a single stimulus is applied [3,4]. Since this interval is on the order of 1% of the reentrant period, hitting it clearly requires precise timing, suggesting that termination due to a single stimulus is difficult to accomplish experimentally or clinically. Indeed, this agrees with clinical findings that termination of reentry by a single stimulus is a rare event [5].

Computer simulations have shown that by injecting two stimuli, the vulnerable window of termination may be greatly increased to as much as tens of milliseconds [6]. This increase in the vulnerable window was caused by two different mechanisms. In both mechanisms, the second stimulus produces a wave that blocks in the retrograde direction only, such that transiently two anterograde waves coexist in the reentrant loop. These anterogradely propagating waves may both block the first time they enter the region close to the stimulus site where the retrograde wave blocked, resulting in a "collision block." Alternatively, they may both cycle for multiple rotations, creating an alternating sequence of long-short action potential duration, eventually causing conduction block and termination ("alternans amplification") [6]. Such conduction block of the anterograde wave, as well as transient double-wave reentry, has been observed experimentally as mechanisms of termination for reentry around a fixed obstacle [7,8].

The antitachycardia pacing modality of implantable cardioverter defibrillators, which delivers one or more trains of stimuli, successfully terminates reentrant tachycardia in most attempts [9,10]. The mechanism underlying such termination is generally thought to be unidirectional block. In some experiments, unidirectional block and subsequent termination of reentry have been observed after the application of several stimuli [7,11], suggesting that the injection of multiple stimuli increases the vulnerable window for unidirectional block. In some cases [7], the first stimuli induced cycle-length oscillations, suggesting that rapid pacing induces dynamical heterogeneity, which in turn establishes the conditions for unidirectional block. However, the exact mechanism of how this may work has not been demonstrated.

We decided to investigate this mechanism in a model system and found that premature stimuli induce spatiotemporal gradients in refractoriness that govern whether subsequent conduction block occurs. In particular, we show that (1) the sign of this gradient at the stimulus site determines whether there is block in the retrograde or in the anterograde direction, (2) this sign alternates such that it is negative for odd stimuli and positive for even stimuli, and (3) the window of block is increased beyond 1–2 ms when the gradient is above a certain critical value (~20 ms/cm). Finally, we introduce a pacing strategy (aggressive ramp), which, in this model, increases the vulnerable window for termination compared to the ramp and burst protocols typically employed in the implantable cardioverter defibrillator.

II. THEORETICAL PREDICTIONS OF SPATIAL GRADIENTS IN RECOVERY TIME

The classic example of unidirectional (anterograde) block due to a single (well-timed) stimulus occurs because the ex-

citable tissue in the direction retrograde to the reentrant wave has had slightly more time to recover from excitation than the tissue in the anterograde direction. This break of spatial symmetry arises because the reentrant front propagates in one direction. Therefore, as a reentrant wave passes the stimulus site, there is a vulnerable time window in which tissue in the retrograde direction has come out of refractoriness, while tissue in the anterograde direction is still refractory. This allows a well-timed stimulus to produce a new wave, which can propagate only in the retrograde direction. If the stimulus is applied earlier, it fails to propagate in either direction, and if it is applied after the vulnerable window, bidirectional propagation occurs.

Insights into the dynamics of the recovery time [termed the diastolic interval (DI) in cardiac electrodynamics] and the action potential duration (APD) around the stimulus site can be obtained by consideration of an analytical approach [12–14], assuming that the APD and the wave-front conduction velocity (CV) are functions of the previous DI. These functional relationships are known as APD and CV restitution curves.

We consider a reentrant wave circulating on a ring geometry with a stimulus site at $x=0$. This reentrant wave is termed F, while waves induced by stimulus number i are termed A_i (for anterograde waves) and R_i (for retrograde waves). Let $t=0$ be the time that the reentrant front passes the stimulus site at $x=0$. The timing between subsequent stimuli is given by their coupling intervals (CIs). At $t=CI_1$, the first stimulus is applied. We compute the resulting DI in the anterograde ($x>0$) and the retrograde directions $x<0$ separately.

For $x>0$,

$$\mathrm{DI}_{\mathrm{A}_1}(x) = \mathrm{CI}_1 - \mathrm{APD}_{\mathrm{F}} - \int_0^x \frac{dx'}{\mathrm{CV}_{\mathrm{F}}} + \int_0^x \frac{dx'}{\mathrm{CV}_{\mathrm{A}_1}(x')}, \quad (1)$$

since $\mathrm{APD}_{\mathrm{F}}$ and CV_{F} do not vary with x. (Note that DI_i precedes APD_i and CV_i.) The spatial gradient in the anterograde direction evaluated at the stimulus site is

$$\frac{\partial \mathrm{DI}_{\mathrm{A}_1}(0)}{\partial x} = -\frac{1}{\mathrm{CV}_{\mathrm{F}}} + \frac{1}{\mathrm{CV}_{\mathrm{A}_1}(0)}. \quad (2)$$

For $x<0$, we get

$$\frac{\partial \mathrm{DI}_{\mathrm{R}_1}(0)}{\partial x} = -\frac{1}{\mathrm{CV}_{\mathrm{F}}} - \frac{1}{\mathrm{CV}_{\mathrm{R}_1}(0)}, \quad (3)$$

where the change in sign compared to Eq. (2) reflects the difference in propagation direction between R_1 and F.

The effective DI gradient at the stimulus is therefore

$$\frac{\partial \mathrm{DI}_1(0)}{\partial x} = \frac{1}{2}\left(\frac{\partial \mathrm{DI}_{\mathrm{R}_1}(0)}{\partial x} + \frac{\partial \mathrm{DI}_{\mathrm{R}_1}(0)}{\partial x}\right), \quad (4)$$

$$= -1/\mathrm{CV}_{\mathrm{F}}, \quad (5)$$

where we have used $\mathrm{CV}_{\mathrm{A}_1}(0)=\mathrm{CV}_{\mathrm{R}_1}(0)=\mathrm{CV}_1$. Since the conduction velocity is positive, the DI_1 gradient is negative, reflecting the fact that repolarization occurs a little later in the anterograde than in the retrograde direction due to the propagation direction of the wave. Hence, at a given time, DI_1 will be shorter in the anterograde than the retrograde direction, or, in other words, there is a negative spatial DI gradient at the stimulus site. The negative sign is what allows for unidirectional block in the anterograde direction due to the application of a well-timed stimulus.

The second stimulus is applied at time $t=\mathrm{CI}_1+\mathrm{CI}_2$. For $x>0$, the DI is

$$\mathrm{DI}_{\mathrm{A}_2}(x) = \mathrm{CI}_2 - \mathrm{APD}_{\mathrm{A}_1}(x) - \int_0^x \frac{dx'}{\mathrm{CV}_{\mathrm{A}_1}(x)} + \int_0^x \frac{dx'}{\mathrm{CV}_{\mathrm{A}_2}(x')}, \quad (6)$$

and the spatial gradient is

$$\frac{\partial \mathrm{DI}_{\mathrm{A}_1}(0)}{\partial x} = -\frac{\partial \mathrm{APD}_{\mathrm{A}_1}(0)}{\partial x} - \frac{1}{\mathrm{CV}_{\mathrm{A}_1}(0)} + \frac{1}{\mathrm{CV}_{\mathrm{A}_2}(0)}, \quad (7)$$

$$= -\frac{da(\mathrm{DI}_1(0))}{d\mathrm{DI}}\frac{\partial \mathrm{DI}_1(0)}{\partial x} - \frac{1}{\mathrm{CV}_1} + \frac{1}{\mathrm{CV}_2}, \quad (8)$$

where $a(\mathrm{DI})$ is the APD restitution curve. Because of the symmetry of the wave propagation around the stimulus site, this equation also holds for $x<0$, so that

$$\frac{\partial \mathrm{DI}_2(0)}{\partial x} = -\frac{da[\mathrm{DI}_1(0)]}{d\mathrm{DI}}\frac{\partial \mathrm{DI}_1(0)}{\partial x} - \frac{1}{\mathrm{CV}_1} + \frac{1}{\mathrm{CV}_2}. \quad (9)$$

Assuming a monotonically increasing APD restitution curve, the first term is positive. If the APD restitution curve is relatively steep and the CV restitution curve relatively flat then the first term will dominate and give a positive DI gradient. Hence, for two stimuli, Eq. (9) predicts that block may occur in the anterograde direction, which is indeed observed in numerical simulations [6]. This expression also predicts that DI_2 may change more steeply in space than DI_1, if the slope of the restitution curve evaluated at $\mathrm{DI}_1(0)$ is larger than 1. In many models and tissues, this is the case for small values of DI. Such increase in $\partial \mathrm{DI}_2(0)/\partial x$ would, in turn, suggest a larger vulnerable window for conduction block at the stimulus site as observed in previous numerical simulations [6].

In general, for i stimuli, the spatial DI gradient is

$$\frac{\partial \mathrm{DI}_i(0)}{\partial x} = -\frac{da[\mathrm{DI}_{i-1}(0)]}{d\mathrm{DI}}\frac{\partial \mathrm{DI}_{i-1}(0)}{\partial x} - \frac{1}{\mathrm{CV}_{i-1}} + \frac{1}{\mathrm{CV}_i}. \quad (10)$$

This expression shows how successive DI gradients may be amplified by APD restitution, possibly setting the stage for increased windows of block and termination. It also shows that the sign of $\partial \mathrm{DI}_i(0)/\partial x$ may alternate, such that the direction in which unidirectional block occurs may alternate between retrograde and anterograde.

III. NUMERICAL SIMULATIONS OF BLOCK AND TERMINATION

A. Numerical methods

To test these predictions, we performed a series of numerical simulations. We use a simple ring geometry by applying periodic boundary conditions to the standard cable equation,

$$\frac{\partial V}{\partial t} = D\frac{\partial^2 V}{\partial x^2} - \frac{I_{ion} + I_{stim}}{C_m}, \tag{11}$$

where V is the transmembrane potential, $D=1$ cm^2/s is the diffusion constant, and $C_m=1$ $\mu\mathrm{F}/\mathrm{cm}^2$ is the membrane capacitance. I_{stim} is the applied stimulus current density of duration 1 ms and amplitude -400 $\mu\mathrm{A}/\mathrm{cm}^2$ ($\approx$2 times threshold). I_{ion} is the membrane current density given by the flux of ions through ion channels, pumps, and exchangers. We use the recent Shiferaw-Sato-Karma (SSK) model [15] for I_{ion}. In addition to the membrane currents, this model includes a comprehensive description of intracellular Ca^{2+} dynamics, which may contribute significantly to the dynamics during rapid activity. Parameters that were varied in previous studies [15,16] were fixed here at $u=11.3$, $\gamma=1.0$, $\tau_f=30$ ms, and $\tau_q=20$ ms. We used a loop size of 16 cm.

For numerical integration, we used a finite-difference method with forward Euler. The values of the temporal and spatial step sizes were $dx=0.015$ cm and $dt=0.01$ ms. Reentry was initiated by inducing a single propagating wave from one end of a cable with no-flux boundary conditions. Once this wave had propagated away from its initiation site, we switched to periodic boundary conditions, causing a circulating excitation wave. We allowed this reentrant activity to reach a periodic steady state (after 10 s, about 30 rotations); these steady-state variables were then used as initial conditions for all subsequent simulations.

As in the previous section, stimuli were always applied at $x=0$ cm. Definitions of the parameters introduced in the previous section are coupling interval (CI: the time since the crossing of -40 mV on the previous action potential upstroke), action potential duration (APD: the time spent above -40 mV), and diastolic interval (DI: the time spent below -40 mV). The spatial gradient of DI ($\partial \mathrm{DI}/\partial x$) at the stimulus site was computed as the difference in DI over a 0.3 cm region centered around $x=0$ cm. Conduction block in a given direction away from the stimulus site was said to occur when the induced wave traveled less than 2 cm.

B. Reentrant activity and one stimulus termination

With a loop size of 16 cm, the SSK model supports a stably rotating action potential wave with a rotation time of 347 ms. From Eq. (5), this gives a value for $\partial \mathrm{DI}_1(0)/\partial x$ of -22 ms/cm, which is also what we find in our simulations. Application of a single premature stimulus causes termination due to unidirectional block of the anterograde wave when delivered in the interval $203.1 \leq \mathrm{CI}_1 \leq 204.5$ ms. Stimuli delivered earlier than this vulnerable window do not induce propagating waves in either the retrograde or the anterograde directions, while stimuli applied later cause phase resetting of the reentry rather than termination [2].

In the following, we first present the results from applying two or three stimuli, systematically varying their timing. Next, we tested the two pacing protocols most commonly used in the implantable cardioverter defibrillator and, finally, we present a pacing strategy that causes short DI values in order to amplify $\partial \mathrm{DI}/\partial x$.

C. Two-stimuli termination

Previous studies have shown that when two stimuli are applied to an ionic ring model (using a modified Beeler-Reuter cell model), two termination mechanisms other than classic unidirectional block may be observed [6,14]. The occurrence of these termination modes were hypothesized to depend on the APD and CV restitution properties (APD and CV are increasing functions of the previous DI) and hence should robustly manifest in ionic models with these properties. The more complex SSK model has considerable memory, such that these functional relationships are more approximate. However, when delivering two premature stimuli such that the first one leads to resetting, we observed those two different types of termination, depending on the timing of the stimuli (i.e., their coupling intervals CI_1 and CI_2).

The first mechanism is called collision block [6] and its dynamics are shown in Figs. 1(a) and 1(b). Initially, there is a single reentrant wave circulating the ring (marked "F" in Fig. 1). Two rotations are shown before delivery of the first stimulus at time $t=1198$ ms. This stimulus triggers a wave in the retrograde direction ("R_1"), which collides with and annihilates the original reentrant front. It also triggers a wave in the anterograde direction ("A_1"), which resets the reentrant activity. The second stimulus (delivered at $t=1378$ ms) blocks in the retrograde direction but propagates successfully in the anterograde direction. Using the notation of Ref. [6], we write this as $\mathrm{R}_2\dashv$ and $\mathrm{A}_2\rightarrow$. At $t\approx 1550$ ms, A_1 runs into the back of R_2 and blocks (since block occurs after one rotation around the ring, this is denoted $\mathrm{A}_1^1\dashv$). However, just prior to colliding with R_2, A_1 encounters tissue that was not activated by R_2 and which, therefore, has longer recovery time (DI) than the surrounding tissue. This in turn causes the wave duration (APD) of A_1 to increase at this location due to APD restitution. This region of increased APD sets up the stage for block of A_2 ($\mathrm{A}_2^1\dashv$), which occurs at $t\approx 1650$ ms. Thus, in short, collision block occurs when R_2 blocks, and A_1 and A_2 subsequently block as they first enter the region where R_2 is blocked. Hence, collision block requires both local (or "type-I" [13]) block and nonlocal (or "type-II" [13]) block.

The other type of termination occurring with two stimuli is termed alternans amplification [6]. This type of termination is also set up by block of R_2 close to the stimulus site, but here neither A_1 nor A_2 block after their first rotation [Figs. 1(c) and 1(d)]. Instead, there is a transient double-wave reentry with A_1 and A_2 corotating. However, this rapid activity causes substantial heterogeneity in DI and APD and head-to-tail interactions between the two waves. In particular, around the stimulus site there are APD and DI alternans

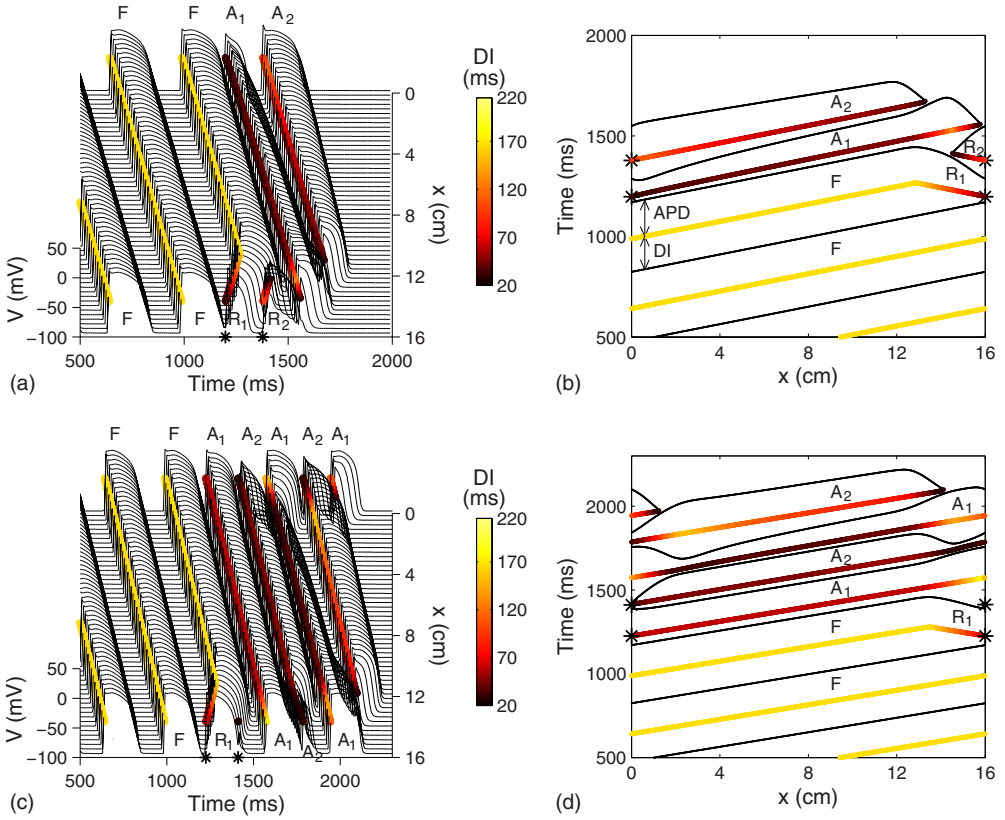

FIG. 1. (Color online) Two-stimulus termination. (a) and (b) Collision block. $CI_1=210$ ms and $CI_2=180$ ms. (a) Transmembrane potential (V) and color-coded DI as function of space and time. (b) Time of occurrence of wave fronts (color-coded for DI) and wave backs (black). Notice that space and time have been reversed compared to panel (a) to provide a more typical space-time plot. Color bar applies to both (a) and (b). Asterisks indicate stimulus times. (c) and (d) Transient double-wave reentry with alternans amplification leading to termination. $CI_1=237$ ms and $CI_2=186$ ms.

of very large amplitude, as well as steep spatial gradients in APD and DI. A_1 blocks after two rotations ($A_1^{2\dashv}$) at a region of increasing APD for A_2 ($x\approx 0.5$ cm, $t\approx 2100$ ms). A_2 also blocks after close to two rotations ($A_2^{2\dashv}$), but at a region of increasing APD for A_1 ($x\approx 12$ cm, $t\approx 2100$ ms).

In our simulations, termination due to collision block occurred much more often, as a function of CI_1 and CI_2 than termination due to alternans amplification. We determined the size of these windows of termination by systematically varying CI_1 and CI_2 in steps of 1 ms. The result is shown in Fig. 2(a). The light gray bar at $CI_1=204$ ms represents termination due to unidirectional block by a single stimulus, while the darker gray dots represent termination due to two stimuli. Collision block ($\{A_1^{1\dashv}, A_2^{1\dashv}\}$) occurs for CI_1 in the range 205–226 ms when CI_2 is within the 170–190 ms range (smaller for large CI_1). In contrast, alternans amplification block occurs in a narrow band (CI_2 width ≈ 1 ms) for CI_1 values of 235–239 ms.

As mentioned above, both collision block and alternans amplification occur in cases where the second stimulus (S2) blocks in the retrograde direction only. The boundary between successful R_2 conduction vs R_2 block is shown as the solid line in Fig. 2(a). When CI_2 is sufficiently short, A_2 also blocks. The dashed line shows the boundary between A_2 conduction and A_2 block. There is a large window of R_2 block and A_2 propagation ($\{R_2\dashv, A_2\rightarrow\}$) for small CI_1. The window of collision block is located within this region. For $CI_1>226$ ms, the $\{R_2\dashv, A_2\rightarrow\}$ window has shrunk to a CI_2 width of around 1 ms; the alternans amplification region is located within this band. For $CI_1>239$ ms, the $\{R_2\dashv, A_2\rightarrow\}$ window has diminished to less than 1 ms (solid and dashes lines overlie each other). These results obtained using the recent SSK model are very similar to those reported previously using the less sophisticated modified Beeler-Reuter ionic cell model [6,14].

As predicted by our analytical approach, $\partial DI_2(0)/\partial x$ (i.e., the gradient that S2 encounters) is positive [Fig. 2(b)], favoring R_2 block. Except for very small CI_1 values, $\partial DI_2(0)/\partial x$ decreases with increasing CI_1, i.e., less premature stimuli tend to cause a smaller gradient, as expected. Indeed, for the more premature stimuli ($CI_1<226$ ms), the amplitude of $\partial DI_2(0)/\partial x$ exceeds that of $\partial DI_1(0)/\partial x$ (22 ms/cm).

The amplitude of $\partial DI_2(0)/\partial x$ correlates well with the size of the $\{R_2\dashv, A_2\rightarrow\}$ window [Fig. 2(c) (open symbols)]. For sufficiently small $\partial DI_2(0)/\partial x$, the $\{R_2\dashv, A_2\rightarrow\}$ window is very small (less than 1 ms or 2 ms). However, for $\partial DI_2(0)/\partial x$ values above a critical threshold value of 20 ms/cm, there is a much larger $\{R_2\dashv, A_2\rightarrow\}$ window, which is tightly correlated with $\partial DI_2(0)/\partial x$, except for the special cases of very short CI_1.

Interestingly, the size of the collision block window ($A_1\dashv, A_2\dashv$) depends on $\partial DI_2(0)/\partial x$ in a very similar manner

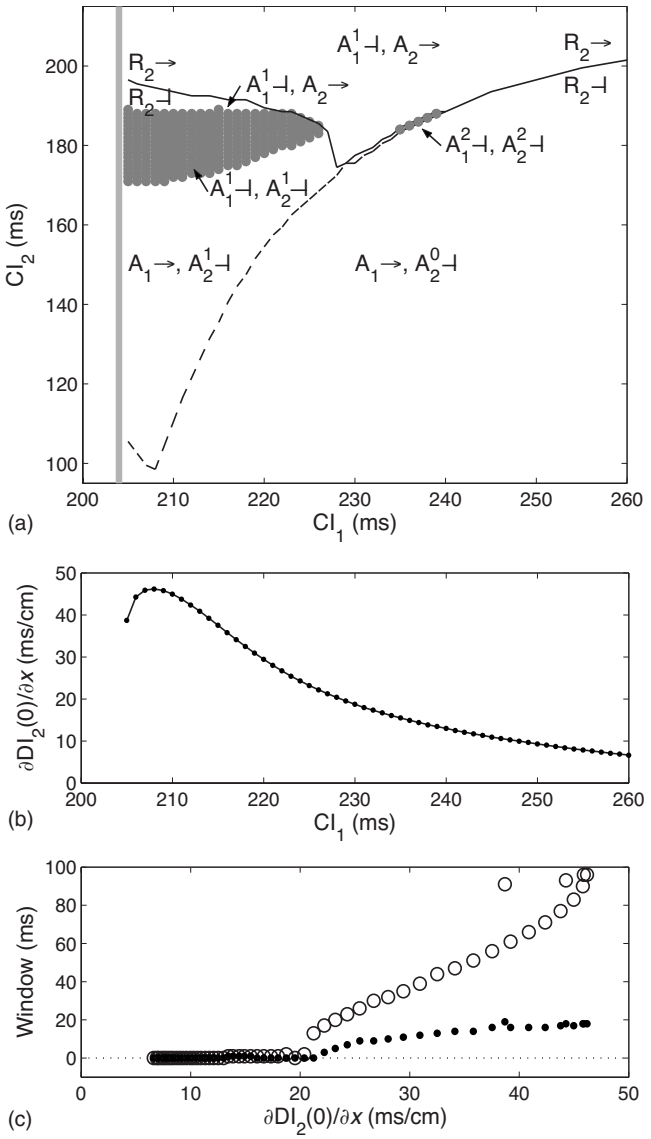

FIG. 2. (a) Termination of reentry due to one (light gray) or two (darker gray) stimuli. Lines indicate borders of conduction block (dashed: A_2 block; solid: R_2 block). (b) Spatial gradient at $x=0$ in DI_2. (c) Correlation between $\partial DI_2(0)/\partial x$ and the size of the $\{R_2\dashv, A_2\rightarrow\}$ window (open circles) and the window of termination (dots).

[Fig. 2(c) (dots)]; below 20 ms/cm there is only a tiny (<1 ms) window of termination, while for $\partial DI_2(0)/\partial x > 20$ ms/cm the size of the termination window increases with $\partial DI_2(0)/\partial x$.

From Fig. 2 it is clear that in this model (as was the case for the Beeler-Reuter model [6]), block of R_2 is a necessary—but not sufficient—condition for collision block. If the second stimulus is applied too early (CI_2 too small), the APD of R_2 is too short to cause block of A_1, which then sustains the reentrant activity. If, on the other hand, the second stimulus is delivered too late (CI_2 too large), even the prolonged APD of A_1 close to the collision site has finished by the time A_2 arrives there, preventing its block. However, although the two premature stimuli do not always cause termination of reentry, they do induce substantial dynamical heterogeneity in APD and DI. In the next section, we investigate how this heterogeneity affects the dynamics following a third premature stimulus.

D. Three-stimuli termination

In order to test the predictions of Eq. (10) and to provide insight into the multiple-stimulus therapies typically used for antitachycardia pacing, we next applied three stimuli. When delivering three premature stimuli, we observe termination due to unidirectional block, where the third stimulus (S3) induces a wave that blocks in the anterograde direction ($A_3\dashv$), but propagates in the retrograde direction ($R_3\rightarrow$). These instances of unidirectional block due to S3 may be preceded by phase resetting with no conduction block due to both S1 and S2 (we term this $\{R_2\rightarrow, A_3\dashv\}$) or preceded by phase resetting due to S1 followed by R_2 block due to S2 (we refer to this as $\{R_2\dashv, A_3\dashv\}$).

Figure 3 shows examples of these two types of termination dynamics. $\{R_2\dashv, A_3\dashv\}$ termination is shown in panels (a) and (b). Here, CI_2 lies within the $\{R_2\dashv, A_2\rightarrow\}$ window of Fig. 2. Hence, for S3 (delivered at $t=1491$ ms), DI_3 is longer in the retrograde direction than in the anterograde direction, causing R_3 to propagate while A_3 blocks. R_3 and A_1 then collide and mutually annihilate, and subsequently A_2 runs into the wave back of A_1 close to this collision site and blocks there.

The $\{R_2\rightarrow, A_3\dashv\}$-type mechanism is shown in Figs. 3(c) and 3(d). Here, CI_2 lies above the region of R_2 block, such that R_2 propagates, collides with, and mutually annihilate A_1. However, because R_2 is preceded by shorter DI_2 values than A_2, it has shorter APD, which in turns increases DI_3 in the retrograde direction, facilitating unidirectional block.

Figure 4(a) gives the vulnerable window for termination in the (CI_1, CI_2, and CI_3) space, while (b) shows the size of the termination window for CI_3 in the (CI_1 and CI_2) plane. Termination due to $\{R_2\dashv, A_3\dashv\}$ is shown in blue hues, while termination due to $\{R_2\rightarrow, A_3\dashv\}$ is shown in red hues. In both (a) and (b), CI_1 and CI_2 were varied in steps of 5 ms, while CI_3 was varied in steps of 1 ms. If termination was not seen with this CI_3 resolution, no data point were added for this (CI_1, CI_2) combination in panel (b) (e.g., at $CI_1=213$ ms, $CI_2=210$ ms). The figure shows that the vulnerable window is larger for the $\{R_2\dashv, A_3\dashv\}$ type, with respect to all CI values (CI_1, CI_2, and CI_3), indicating that unidirectional block is facilitated by prior block of R_2.

Since the spatial DI gradient is negative for S1 and positive for S2, Eq. (10) predicts that it is negative again for S3, which would cause unidirectional block in the retrograde direction as observed. The computed $\partial DI_3(0)/\partial x$ is indeed negative and becomes more so as CI_2 is shortened—i.e., the more premature the stimulus, the steeper the gradient (Fig. 4) in agreement with our analytical findings. In addition, there tends to be a biphasic relationship between $\partial DI_2(0)/\partial x$ and CI_1 for fixed CI_2, with $\partial DI_2(0)/\partial x$ increasing in magnitude with increased CI_1 for shorter CI_1 and decreasing for larger CI_1 values.

The occurrence of unidirectional block and termination increases with the size of the gradient (Fig. 4), as was the

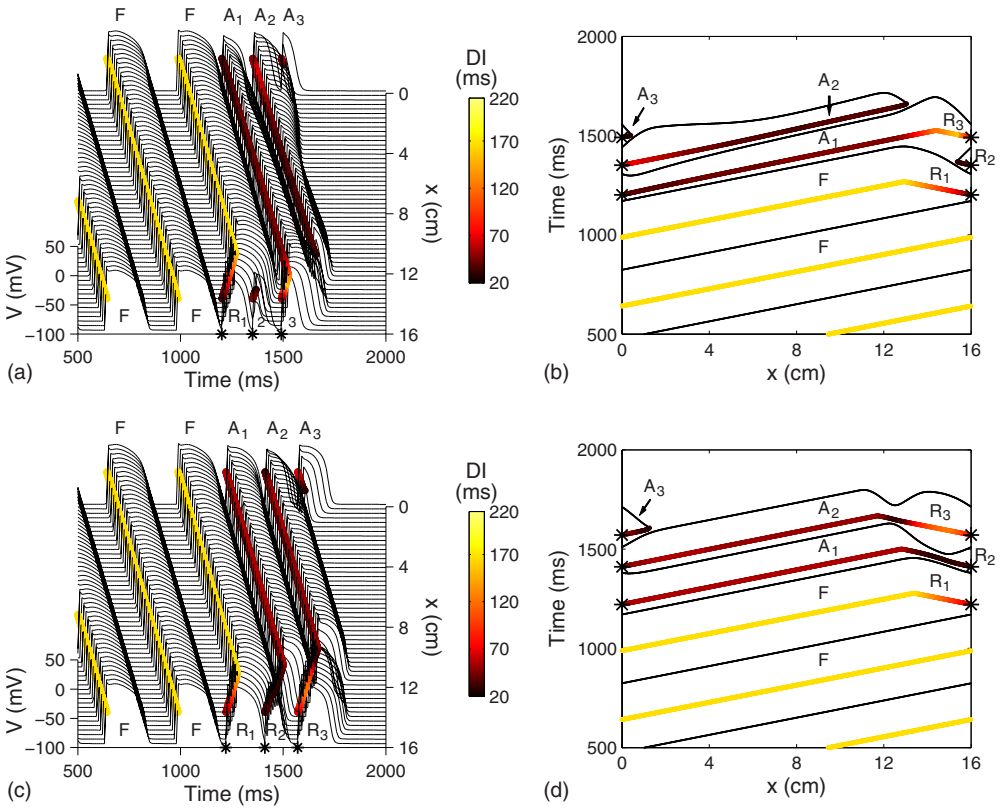

FIG. 3. (Color online) Termination of reentry due to three stimuli. (a) and (b) Termination due to $\{R_2\dashv, A_3\dashv\}$; $CI_1=213$ ms, $CI_2=150$ ms, and $CI_3=140$ ms. "2" and "3" indicate R_2 and R_3, respectively. (c) and (d) Termination of reentry due to $\{R_2\rightarrow, A_3\dashv\}$; $CI_1=233$ ms, $CI_2=190$ ms, and $CI_3=160$ ms.

case for termination due to two stimuli. However, for three stimuli the correlation is less tight, presumably due to memory effects in the ionic model. Again there is a threshold value for the block and termination windows to be larger than 1 ms and, further, the size of this threshold is the same as for the two-stimulus case (20 ms/cm).

In contrast to the dynamics due to two stimuli, where block of R_2 led to reentry termination in only about 30% of the cases, anterograde block (AGB) due to the third stimulus led to termination in most cases (i.e., those where circles and dots are superimposed in Fig. 4). The instances for which anterograde block did not cause termination occurred because R_3 blocked further away from the stimulus site. Hence, the local DI gradient may predict the dynamics at the stimulus site well, but in some cases nonlocal effects lead to an unexpected outcome.

E. Burst pacing

For antitachycardia pacing, the ICD typically employs either a burst pacing protocol with constant coupling intervals or a ramp pacing protocol where coupling intervals decrease by a fixed amount for each stimulus applied. Next, we investigated the mechanisms by which these protocols may lead to reentry termination.

Figure 5(a) shows an example of a burst protocol. In this case, the coupling intervals were 220 ms and 15 stimuli were applied. While the rapid pacing did not cause block in either the retrograde or the anterograde direction, it did induce APD alternans [Figs. 5(a) and 5(b)]. Similar to the three-stimulus protocols discussed above, this burst pacing protocol leads to a negative value of $\partial DI_1(0)/\partial x$ (of -22 ms/cm), a positive gradient for the second beat, and a negative value again for the third beat [Fig. 5(c)]. Indeed, the sign of $\partial DI(0)/\partial x$ alternates throughout the burst protocol as predicted, but its amplitude decreases.

Because we did not observe termination with the burst protocol itself, we decided to investigate the effects of the protocol in setting up DI gradients favorable to termination by a premature stimulus following the burst pacing. Hence, in individual simulations, we applied such premature stimuli, systematically varying its timing and the number of stimuli in the burst. Thus, we determined the window of block and termination following bursts of varying stimulus numbers. The results are shown in Fig. 5(d). There are significant windows of block only when the premature stimulus follows either one stimulus or three stimuli at the burst rate of 220 ms (i.e., when the premature stimulus is beat number two or four, respectively). Due to the alternating sign of $\partial DI(0)/\partial x$, in both of these cases, $\partial DI(0)/\partial x$ is positive and the conduction block is of the retrograde wave. As discussed above, this does not always lead to reentry termination. In the cases where reentry was terminated, this was due to collision block.

When applying a more rapid burst protocol with coupling intervals of 215 ms, the DI and APD alternans amplitude increases [Figs. 6(a) and 6(b)]. While the sign of $\partial DI(0)/\partial x$

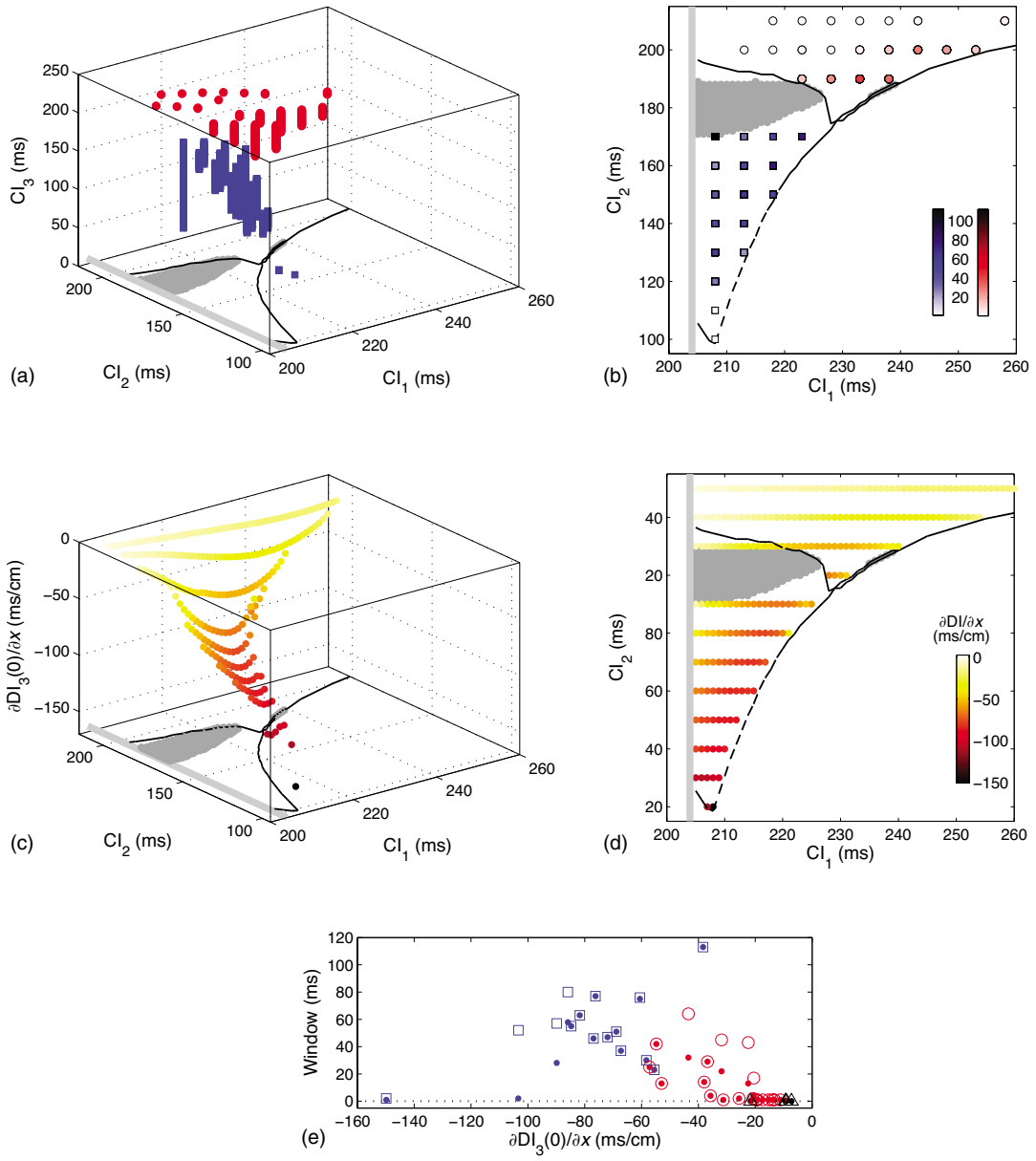

FIG. 4. (Color online) Vulnerable window of reentry termination [(a) and (b)] and DI gradient [(c and d)] with three stimuli. (a) CI_1, CI_2, and CI_3 combinations causing termination due to $\{R_2\dashv, A_3\dashv\}$ [blue (dark gray) squares] and $\{R_2\rightarrow, A_3\dashv\}$ [red (light gray) circles]. (b) Projection onto CI_1 and CI_2 planes, color-coded according to the size of CI_3 termination window (in ms). (c) and (d) Gradient in DI_3 at $x=0$ ($\partial DI_3(0)/\partial x$) shown as a function of CI_1 and CI_2. (d) Projection onto CI_1 and CI_2 planes. (e) Correlation between DI_3 gradient and windows for unidirectional block (open symbols) and termination (dots). Colors and symbols indicate different dynamics: $\{R_2\dashv, A_3\dashv\}$ [blue (dark gray) squares], $\{R_2\rightarrow, A_3\dashv\}$ [red (light gray) circles], and $A_3\rightarrow$ (black triangles).

also alternates, its amplitude decreases with time [Fig. 6(c)] as was the case in Fig. 5. Again, the burst protocol by itself does not cause conduction block or reentry termination, but it does induce spatiotemporal heterogeneity in DI so that premature stimuli delivered immediately after the burst may cause termination [Fig. 6(d)]. Termination always occurs after block of the retrograde wave on even beats, where $\partial DI(0)/\partial x > 0$. The termination dynamics of the two remaining anterograde waves vary with the stimulus number. Following S2 and S4, there is regular collision block ($\{A^1_{i-1}\dashv, A^1_i\dashv\}$), S8 and S10 lead to $\{A^2_{i-1}\dashv, A^1_i\dashv\}$ termination, while small (>3 ms) windows of $\{A^2_{i-1}\dashv, A^2_i\dashv\}$ and $\{A^3_{i-1}\dashv, A^3_i\dashv\}$ termination exists for beats 12 and 6, respectively.

While the type of termination dynamics is not predictable by the local DI gradient, the occurrence of block is (Fig. 7). As stated above, the rapid burst protocols induce considerably large positive DI gradients, which lead to retrograde block (RGB). However, the threshold value for $\partial DI(0)/\partial x$ to cause block depends on the burst timing. For coupling intervals of $CI_j = 220$ ms, the threshold value is between 10 and 17 ms/cm (gray symbols in Fig. 7), while for $CI_j = 215$ ms, it is close to zero (orange symbols). For $CI_j = 240$ ms, the larg-

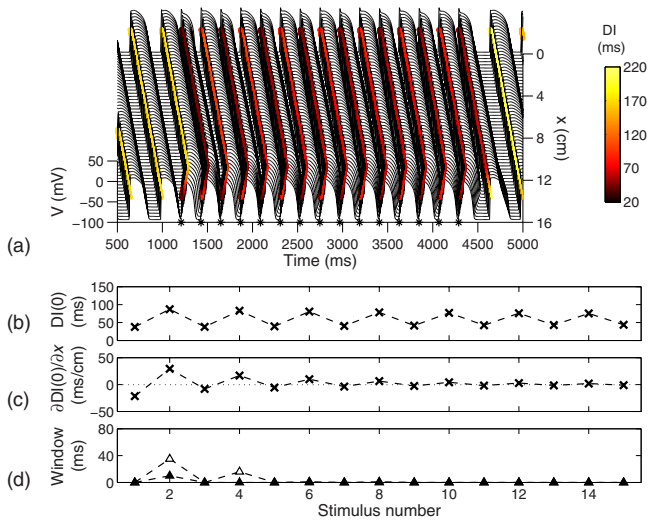

FIG. 5. (Color online) Dynamics due to burst pacing with coupling intervals of 220 ms. (a) Transmembrane potential and DI. (b) Successive values of DI at the stimulus site. (c) Spatial DI gradient at the stimulus site. (d) Windows of block and termination. Retrograde block (open triangles) and retrograde block causing termination (filled triangles).

est positive value of $\partial \mathrm{DI}(0)/\partial x$ was 13 ms/s and no block occurred (black symbols).

F. Ramp pacing

We next studied the effects of ramp pacing protocols where consecutive coupling intervals are decreased by a fixed amount ΔCI. Figure 8 shows the ensuing dynamics for the case of $\Delta\mathrm{CI}=30$ ms. Hence, $\mathrm{CI}_1=T_0=347$ ms (where T_0 is the period of the unperturbed reentry), $\mathrm{CI}_2=T_0-\Delta\mathrm{CI}$

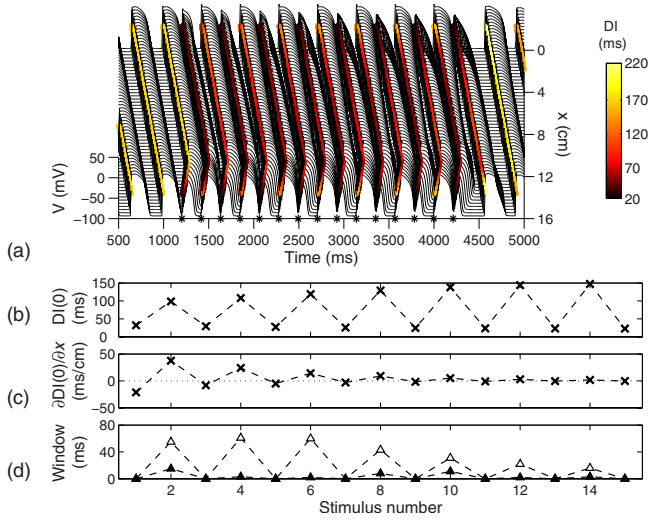

FIG. 6. (Color online) Dynamics due to burst pacing with coupling intervals of 215 ms. (a) Transmembrane potential and DI. (b) Successive values of DI at the stimulus site. (c) Spatial DI gradient at the stimulus site. (d) Windows of block and termination. Retrograde block (open triangles) and retrograde block causing termination (filled triangles).

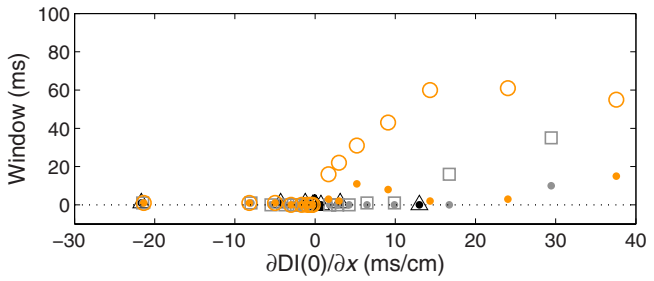

FIG. 7. (Color online) Correlation between vulnerable window for termination (dots) and block (open symbols) and local DI gradient. Data points are from all beats in burst protocols with $\mathrm{CI}_j=215$ ms [orange (light gray) circles], $\mathrm{CI}_j=220$ ms (gray squares), and $\mathrm{CI}_j=240$ ms (black triangles).

$=317$ ms, $\mathrm{CI}_3=T_0-2\Delta\mathrm{CI}=287$ ms, etc. This shortening of CI leads to a shortening of DI [Fig. 8(b)], but no wave block or termination occurs until eventually the eighth stimulus falls within the refractory period and is unable to induce waves in either direction. To quantify the ability of the ramp protocol to cause block and termination, we applied premature stimuli S1–S7 or a postmature S8. There is little heterogeneity at the stimulus site for the first seven beats [Fig. 8(c)], but when S8 is applied there is a positive DI gradient, causing block of the retrograde wave but no subsequent termination [Figs. 8(c) and 8(d)].

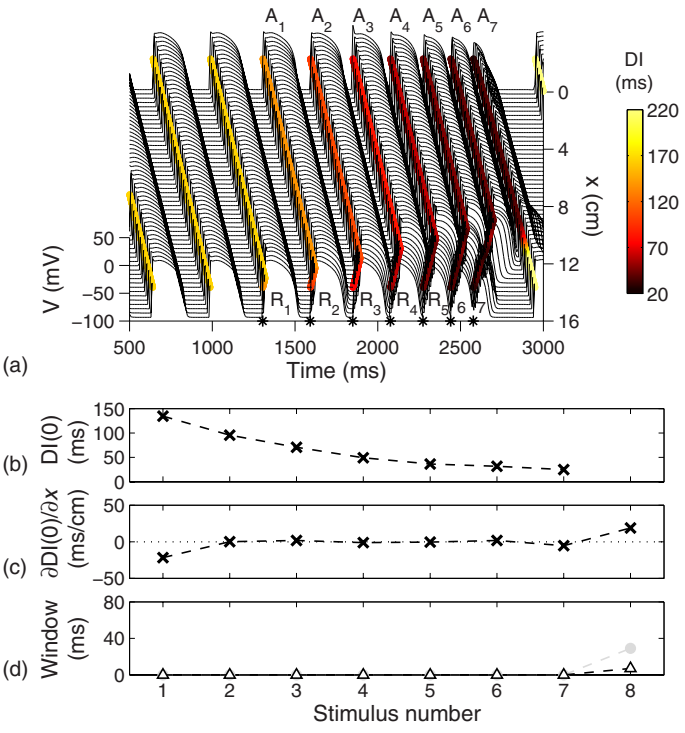

FIG. 8. (Color online) Dynamics due to ramp pacing with an interstimulus decrement of 30 ms. (a) Transmembrane potential and DI. (b) Successive values of DI at the stimulus site. (c) Spatial DI gradient at the stimulus site. (d) Windows of block and termination. Retrograde block (open triangles), retrograde block causing termination (filled triangles), and nonlocal block leading to termination (gray circles).

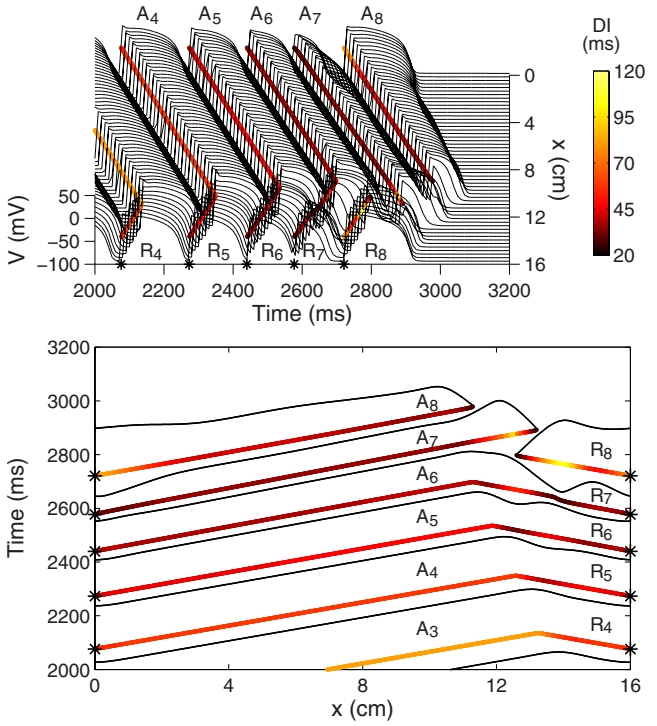

FIG. 9. (Color online) Termination due to nonlocal DI fluctuations following a ramp protocol (S1–S7 with ΔCI=30 ms) with a postmature stimulus (S8).

However, there is a significant window of termination due to nonlocal conduction block [gray symbol in Fig. 8(d)]. This occurs as the progressive shortening of the CI allows waves to travel further and further in the retrograde direction before colliding with the anterograde waves (Fig. 9). This causes each retrograde wave to reach an area beyond the collision point of the previous waves where DI is prolonged due to CV restitution effects (because the anterograde waves travel further than the retrograde waves, CV restitution effects accumulate more there). These increasing fluctuations in DI and APD (through APD restitution) eventually cause R_8 to block, with subsequent block of A_7 and $A_8(\{A_7^{1\dashv}, A_8^{1\dashv}\})$ in a manner reminiscent of collision block [Figs. 1(a) and 1(b)].

Other values of ΔCI (10, 20, and 40 ms) resulted in very small (less than 2 ms) windows of termination.

G. Aggressive ramp pacing

One of the predictions based on Eq. (10) is that APD restitution may amplify successive spatial DI gradients at the stimulus site, if the slope of the APD restitution curve is larger than one, which is the case for short DI values for this model. When applying the rapid burst protocols, DI is short only for every other beat (Figs. 5 and 6). For the ramp protocols, DI is initially quite large such that DI is very homogeneous at the stimulus site.

We hypothesized that a more efficient way to induce conduction block and reentry termination would be to apply a protocol with an initial short CI (CI_1) followed by a ramp series with increasingly shorter values of CI. Hence, $CI_2 = CI_1 - \Delta CI$, $CI_3 = CI_1 - 2\Delta CI$, etc., such that by shortening the initial CI, subsequent CI values are also decreased. In this way, DI values would be short and fall on the steep part of the APD restitution curve. We refer to this type of protocol as an aggressive ramp.

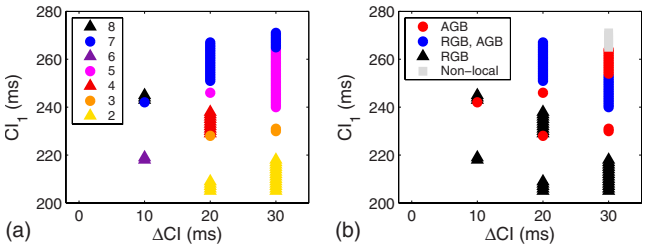

FIG. 10. (Color online) Vulnerable window for termination using an aggressive ramp protocol with different values of the stimulus timing parameters. (a) Color-coded for number of stimuli required for termination. (b) Color-coded according to mechanism of termination: anterograde block (AGB: $\{R_{i-1}\rightarrow, A_i^{\dashv}\}$), anterograde block preceded by retrograde block (RGB, AGB: $\{R_{i-1}^{\dashv}, A_i^{\dashv}\}$), retrograde block leading to collision block (RGB: $\{A_{i-1}^{1\dashv}, A_i^{1\dashv}\}$, or nonlocal block preceded by bidirectional block).

We performed a series of simulations in which we varied systematically CI_1 and ΔCI. Indeed, the aggressive ramp protocol caused reentry termination for a range of these stimulus timing parameters (Fig. 10). Depending on these parameters, various numbers of stimuli caused wave block [Fig. 10(a)] and different types of termination mechanisms occurred [Fig. 10(b)]. Anterograde block always occurred for an odd number of stimuli. In some cases, anterograde block was preceded by retrograde block, which took place for an even number of applied stimuli. Finally, for some parameter combinations, retrograde block by itself caused termination using an even number of stimuli (due to collision block).

In order to investigate this dependence of the wave block occurrence on the stimulus number, we computed the DI gradient and the resulting window of wave block for a range of $(CI_1, \Delta CI)$ combinations. Figure 11(a) shows an example in which S5 encounters a negative DI gradient and causes anterograde block and termination, while Fig. 12(a) shows a case where a positive $\partial DI(0)/\partial x$ for S4 induces retrograde block, succeeded by a negative $\partial DI(0)/\partial x$ for S5 causing retrograde block. Thus, it is clear that the aggressive ramp protocol can induce an amplification in DI heterogeneity, as outlined in Sec. II.

As was the case for the other protocols, there is a strong correlation between $\partial DI(0)/\partial x$ and the window of wave block (Fig. 13). The threshold value for block in the anterograde direction is close to 20 ms/cm. Due to the lack of data points, it is not possible to determine the threshold value for retrograde block, but it is in the range of 25–60 ms/cm.

IV. DISCUSSION

A. Two-stimulus termination

We found that using two stimuli, rather than just one, greatly increases the vulnerable window for termination due to mechanisms other than classic unidirectional block of the anterograde wave (Fig. 2). This finding is very similar to

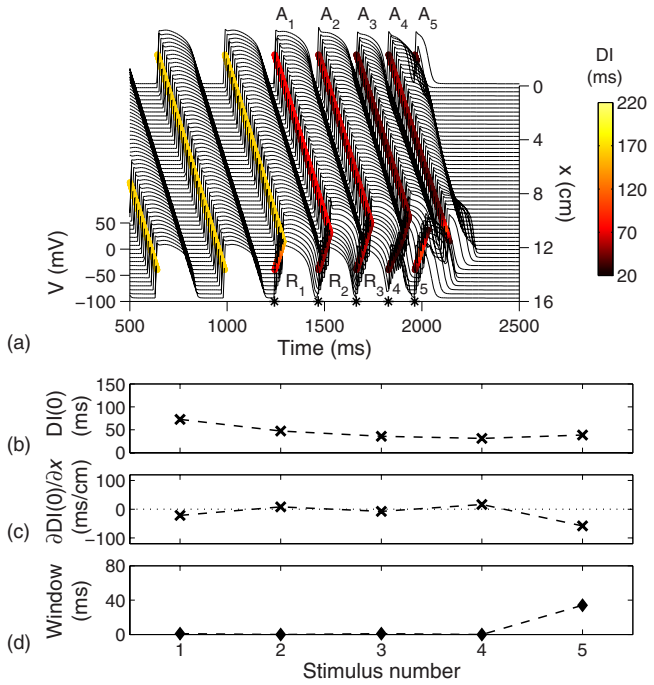

FIG. 11. (Color online) Termination due to unidirectional block in aggressive ramp protocol with $\Delta CI=30$ ms and $CI_1=255$ ms. (a) Transmembrane potential and DI. (b) Successive values of DI at the stimulus site. (c) Spatial DI gradient at the stimulus site. (d) Windows of block and termination. Anterograde block (diamonds).

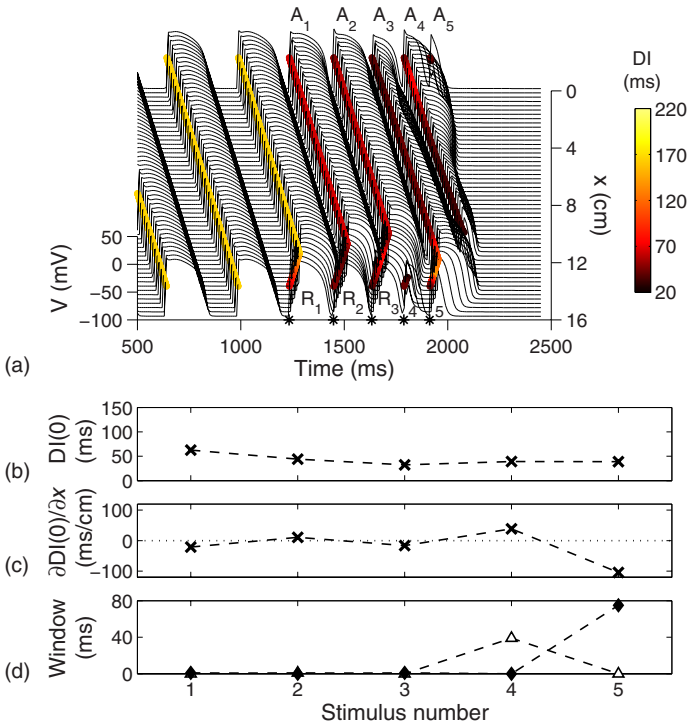

FIG. 12. (Color online) Termination due to unidirectional block preceded by retrograde block in aggressive ramp protocol with $\Delta CI=30$ ms and $CI_1=245$ ms. (a) Transmembrane potential and DI. (b) Successive values of DI at the stimulus site. (c) Spatial DI gradient at the stimulus site. (d) Windows of block and termination. Retrograde block (triangles) and anterograde block (diamonds).

those obtained previously using a different ionic model [6], demonstrating that the results are not particular to a certain ionic model.

The most prevalent mechanism of block due to two stimuli in our simulations was collision block, while alternans amplification occurred for only a narrow range of CI_1 and CI_2 pairs. This is almost certainly due to our ring size being relatively short since the relative occurrence of collision block vs alternans amplification depends on the ring size, with the window for alternans amplification increasing for longer rings and the window for collision block decreasing [14] (in essence, the longer the ring, the easier it is for two waves to coexist).

Both collision block and alternans amplification require the R_2 wave to block. As can be appreciated from Fig. 1, such block requires the APD of R_1 to become increasingly longer away from the stimulus site. In other words, it sets requirements on the APD restitution curve to be sufficiently steep. However, R_2 block also depends on how the conduction velocity changes with DI. If CV restitution is steep, R_2 slows down substantially as it propagates, allowing R_1 more time to repolarize and, thus, decreasing the chance of R_2 block. Hence, the occurrence of R_2 block is increased when APD restitution is steep and CV restitution is flat [14]. We also derive this result in Sec. II.

Collision block and alternans amplification also both require the transient coexistence of two anterograde waves. Such double-wave reentry would effectively cut the activation time in half. Acceleration of ventricular tachycardia is sometimes observed upon delivery of stimuli by an implantable cardioverter defibrillator [10,17–19]. Such acceleration may be due to additional wave fronts, speed up of a single wave, change in pathway for a single wave, or combinations hereof. Hence, while it may be premature to suggest a transient double-wave reentry as the cause of the increased activation in the *in situ* heart, double-wave reentries have been observed in experimental systems in response to rapid pacing [7,20].

B. Gradient in refractoriness

Ironically, there are important similarities between termination and initiation of cardiac reentry. The establishment of

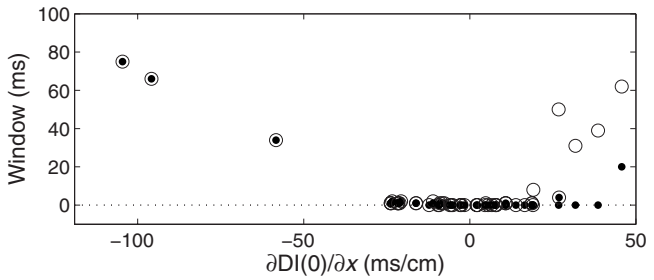

FIG. 13. Correlation between block, termination, and local DI gradient for the aggressive ramp protocol. Data points were obtained from all beats of aggressive ramp protocols with nine different parameter settings: combinations of $\Delta CI=10$, 20, and 30 ms and $CI_1=230$, 245, and 255 ms.

unidirectional conduction block as a necessary condition for the onset of reentry occurred almost 100 years ago [21], but conduction block also plays a pivotal role in annihilating ongoing reentry. Since gradients in refractoriness are known to be critical determinants for conduction block and the onset of reentry and/or arrhythmias [22–28], we had hypothesized that such gradients also play a major role in pacing-induced reentry termination.

With the exception of one of the burst protocols (Fig. 7), we found that the vulnerable window for conduction block exceeds 1–2 ms only when the size of the DI gradient is larger than ~20 ms/cm. This value is very similar to those seen for conduction block due to a single stimulus in heterogeneous cables [29,30] and comparable in size to the wide range of values (10–120 ms/cm) reported from *ex vivo* studies using a variety of experimental preparations and conditions [22–25].

This critical value of this gradient depends on the CV restitution properties of the tissue [13,29]. Theoretical studies have given the following sufficient, but not necessary condition for conduction block [13,31]:

$$dt_r/dx > 1/\mathrm{CV}_{min}, \tag{12}$$

where t_r is the repolarization time and CV_{min} is the CV of the smallest possible DI value that allows conduction. In our simulations, we observe $\mathrm{CV}_{min} \approx 30$ cm/s, which suggests the blocking condition [Eq. (12)] to be $dt_r/dx > 30$ ms/cm. This value is surprisingly close to our estimate given that it guarantees block at some distance, whereas we are concerned with block close to the stimulus site.

The phenomenon of amplification of spatial heterogeneity in action potential parameters through steep APD restitution that we observe here has also been described for block at a distance in cardiac fibers [13], further linking the occurrence of conduction block in a fiber and unidirectional block on the ring.

C. Mechanisms of termination due to three and more stimuli

By applying three stimuli, we found a much increased vulnerable window for unidirectional block for the third stimulus (Fig. 4). The first two premature stimuli cause a negative spatial DI gradient, which can be much larger in amplitude (>100 ms/cm; Fig. 4) than that due to the first stimulus alone (<50 ms/cm; Fig. 2). By creating this heterogeneity, the first two stimuli in the sequence establish tissue for anterograde block. We found that the main facilitator of anterograde block is block of R_2, but formation of R_2 waves with a short APD also promotes it. Both of these conditions are in turn facilitated by steep APD restitution.

That earlier stimuli may augment the occurrence of conduction block has been shown in previous cable simulation studies [13,30,32] and experimental studies [25,28,33]. Also, in the clinic, delivery of multiple stimuli increases the termination success rate [34]. Here, we show that on the ring, an odd number of stimuli specifically increase the window for block of the anterograde wave, leading to termination of reentry, while an even number of stimuli may increase the occurrence of retrograde block. When applying trains of up to seven stimuli with random timing (not shown), we did not observe any new types of termination mechanism, suggesting that those described here and previously (i.e., unidirectional block of the anterograde wave, collision block, and alternans amplification) suffices to explain multistimulus pacing termination of reentry in simple geometries and, potentially, antitachycardia pacing in the *in situ* heart.

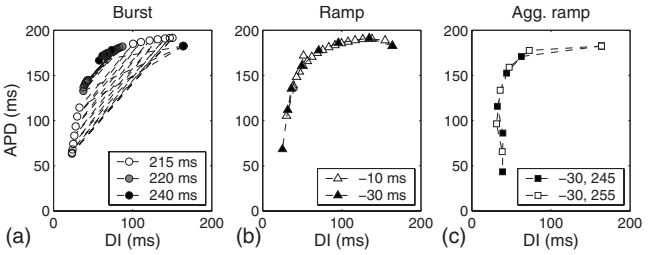

FIG. 14. APD restitution curves. (a) From burst protocols with three different coupling intervals. (b) From ramp protocols with two different ramp decrements. (c) From aggressive ramp protocol with two different initial step sizes.

D. Termination of alternating reentry

Rapid activation typically induces repolarization alternans, which we see with the burst pacing when the coupling intervals are 215 ms or 220 ms (Figs. 6 and 5). Previous studies have suggested that the occurrence of alternans due to a short reentrant path increases the vulnerable window for termination [35–37]. In the present model, where the alternans are not caused by a short reentrant pathway, but due to rapid external pacing from the stimulus site, we find that although the alternans is spatially discordant and DI varies along the ring, the presence of such alternans does not increase the ability to terminate the reentry because the DI gradient around the stimulus site is small (Fig. 6), preventing unidirectional block.

E. Aggressive ramp and implications for antitachycardia pacing

In our model, the aggressive ramp protocol works well because—by design—the DI values fall on the steep part of the APD restitution curve (Fig. 14). Hence, it may be that an as-soon-as-possible pacing scheme where all coupling intervals were just beyond the refractory period would increase the termination efficacy even more; but such an approach would be difficult to implement in an implantable device given that the APD restitution curve is a dynamic property and depends on the state of the heart (e.g., heart rate, sympathetic activity, etc). In contrast, the aggressive ramp has only two parameters, which do not need fine tuning (Fig. 10).

While in our simple model, we found no or very little termination when applying regular burst or ramp pacing, these protocols actually work relatively well in patients. This discrepancy may be due to intrinsic structural and ionic heterogeneity as well as anisotropy in the heart and/or the lack of a reentrant pathway in the heart as well defined as our loop. Given that our model appears to underestimate the efficacy of these traditional antitachycardia pacing algorithms,

it may well be that the aggressive ramp may work even better than the predictions here suggest. In particular, it would be of interest to test the aggressive ramp protocol for termination of spiral waves, for which other annihilation types have been proposed (e.g., unpinning due to an applied field [38,39]) in addition to unpinning due to burst pacing [40]. However, while the aggressive ramp protocol needs to be tested in a two-dimensional, heterogeneous, anisotropic, and scarred tissue, we feel that these simulations in the simple ring model are a promising step.

ACKNOWLEDGMENTS

This work was supported by the NSF (Grant No. PHY-0513389) and the Kenny Gordon Foundation.

[1] N. Wiener and A. Rosenblueth, Arch. Inst. Cardiol. Mex **16**, 205 (1946).
[2] L. Glass and M. E. Josephson, Phys. Rev. Lett. **75**, 2059 (1995).
[3] C. F. Starmer, V. N. Biktashev, D. N. R. M. R. Stepanov, O. N. Makarova, and V. I. Krinsky, Biophys. J. **65**, 1775 (1993).
[4] R. M. Shaw and Y. Rudy, J. Cardiovasc. Electrophysiol. **6**, 115 (1995).
[5] M. J. Gardner, H. L. Waxman, A. E. Buxton, M. E. Cain, and M. E. Josephson, Am. J. Cardiol. **50**, 1338 (1982).
[6] P. Comtois and A. Vinet, Chaos **12**, 903 (2002).
[7] L. Boersma, J. Brugada, C. Kirchhof, and M. Allessie, Circulation **88**, 1852 (1993).
[8] B. Mensour, E. Jalil, A. Vinet, and T. Kus, Pacing Clin. Electrophysiol. **23**, 1200 (2000).
[9] A. Schaumann, F. von zur Muhlen, B. Herse, B. D. Gonska, and H. Kreuzer, Circulation **97**, 66 (1998).
[10] R. Fries, A. Heisel, G. Kalweit, J. Jung, and H. Schieffer, Pacing Clin. Electrophysiol. **20**, 198 (1997).
[11] P. A. Boyden, L. H. Frame, and B. F. Hoffman, Circulation **79**, 406 (1989).
[12] J. W. Cain, E. G. Tolkacheva, D. G. Schaeffer, and D. J. Gauthier, Phys. Rev. E **70**, 061906 (2004).
[13] N. F. Otani, Phys. Rev. E **75**, 021910 (2007).
[14] P. Comtois and A. Vinet, Chaos **17**, 023125 (2007).
[15] Y. Shiferaw, D. Sato, and A. Karma, Phys. Rev. E **71**, 021903 (2005).
[16] Y. Shiferaw, M. A. Watanabe, A. Garfinkel, J. N. Weiss, and A. Karma, Biophys. J. **85**, 3666 (2003).
[17] S. C. Hammill, D. L. Packer, M. S. Stanton, J. Fetter, and M. P. I. GROUP, Pacing Clin. Electrophysiol. **18**, 3 (1995).
[18] M. S. Wathen, M. O. Sweeney, P. J. DeGroot, A. J. Stark, J. L. Koehler, M. B. Chisner, C. Machado, W. O. Adkisson, and PainFree Rx Investigators, Circulation **104**, 796 (2001).
[19] R. C. Klein *et al.*, J. Cardiovasc. Electrophysiol. **14**, 940 (2003).
[20] N. Bursac and L. Tung, Cardiovasc. Res. **69**, 381 (2006).
[21] G. K. Mines, J. Physiol. (London) **46**, 350 (1913).
[22] W. B. Gough, R. Mehra, M. Restivo, R. H. Zeiler, and N. el Sherif, Circ. Res. **57**, 432 (1985).
[23] T. Osaka, I. Kodama, N. Tsuboi, J. Toyama, and K. Yamada, Circulation **76**, 226 (1987).
[24] M. Restivo, W. B. Gough, and N. El-Sherif, Circ. Res. **66**, 1310 (1990).
[25] K. Laurita and D. Rosenbaum, Circ. Res. **87**, 922 (2000).
[26] K. J. Sampson and C. S. Henriquez, Chaos **12**, 819 (2002).
[27] A. W. Chow, O. R. Segal, D. W. Davies, and N. S. Peters, Circulation **110**, 1725 (2004).
[28] A. R. M. Gelzer, M. L. Koller, N. F. Otani, J. J. Fox, M. W. Enyeart, G. J. Hooker, M. L. Riccio, C. R. Bartoli, and R. F. Gilmour, Jr., Circulation **118**, 1123 (2008).
[29] K. J. Sampson and C. S. Henriquez, Am. J. Physiol. **281**, H2597 (2001).
[30] Z. Qu, A. Garfinkel, and J. N. Weiss, Biophys. J. **91**, 793 (2006).
[31] P. Comtois, A. Vinet, and S. Nattel, Phys. Rev. E **72**, 031919 (2005).
[32] J. J. Fox, M. L. Riccio, P. Drury, A. Werthman, and R. F. Gilmour, Jr., New J. Phys. **5**, 101.1 (2003).
[33] N. El-Sherif, W. B. Gough, and M. Restivo, Circulation **83**, 268 (1991).
[34] J. M. Almendral, M. E. Rosenthal, N. J. Stamato, F. E. Marchlinski, A. E. Buxton, L. H. Frame, J. M. Miller, and M. E. Josephson, J. Am. Coll. Cardiol. **8**, 294 (1986).
[35] L. H. Frame and M. B. Simson, Circulation **78**, 1277 (1988).
[36] W. Quan and Y. Rudy, Pacing Clin. Electrophysiol. **14**, 1700 (1991).
[37] T. Krogh-Madsen and D. J. Christini, *Proceedings of the 2008 Conference on Frontiers of Applied and Computational Mathematics* (World Scientific, Singapore, 2009).
[38] S. Takagi, A. Pumir, D. Pazó, I. Efimov, V. Nikolski, and V. Krinsky, Phys. Rev. Lett. **93**, 058101 (2004).
[39] C. M. Ripplinger, V. I. Krinsky, V. P. Nikolski, and I. R. Efimov, Am. J. Physiol. Heart Circ. Physiol. **291**, H184 (2006).
[40] Y.-Q. Fu, H. Zhang, Z. Cao, B. Zheng, and G. Hu, Phys. Rev. E **72**, 046206 (2005).